of X_t at the surface of the multilayer by a Debye-Waller factor.

When a multilayer is exactly periodic we can consider the structure as an artificial crystal and calculate the diffraction profile with the formalism of the dynamical theory. For a rectangular composition profile, the complex structure factors which are used in the expressions for η and T are given by (Underwood & Barbee, 1981)

$$\Gamma F_0 = 2(\bar{\delta} + i\bar{\beta}), \tag{55}$$

$$\Gamma(F_H F_{\bar{H}})^{1/2} = 2[\delta_1 - \delta_2 + i(\beta_1 - \beta_2)] \times \sin(m\pi d_1/d)/m\pi, \tag{56}$$

where $\bar{\delta}$ and $\bar{\beta}$ are weighted average values and d_1/d is the volume fraction of the heavy element in a two-layer sequence. Fig. 6 shows Cu $K\alpha_1$ reflection profiles on a logarithmic and a linear scale calculated with the optical and the dynamical theory for a multilayer with 30 periods of 60 Å composed of 15 Å tungsten and 45 Å carbon. Both theories take into account multiple reflections and are in this sense dynamical. However, it must be remembered that the Takagi-Taupin theory is essentially a two-beam theory, which can describe only one reflection at a time and is not valid in the region of total reflection below about 0·3°. This explains the small differences between the two profiles.

The authors thank H.F.J. van 't Blik for the growth of superlattices and B.A.H. van Bakel for the growth of epitaxial layers on InP.

References

BARTELS, W. J. (1983). *J. Vac. Sci. Technol.* B1, 338-345.

BARTELS, W. J. & NIJMAN, W. (1978). *J. Cryst. Growth*, **44**, 518-525.

BONSE, U. & GRAEFF, W. (1977). *X-ray Optics*, edited by H.-J. QUEISSER, pp. 93-143. Berlin: Springer-Verlag.

BORN, M. & WOLF, E. (1980). *Principles of Optics*. Oxford: Pergamon Press.

COLE, H. & STEMPLE, N. R. (1962). *J. Appl. Phys.* **33**, 2227-2233.

DARWIN, C. G. (1914). *Philos. Mag.* **27**, 315-333, 675-690.

EWALD, P. P. (1917). *Ann. Phys. (Leipzig)*, **54**, 519-597.

FINGERLAND, A. (1971). *Acta Cryst.* A**27**, 280-284.

HALLIWELL, M. A. G., LYONS, M. H. & HILL, M. J. (1984). *J. Cryst. Growth.* **68**, 523-531.

HILL, M. J., TANNER, B. K., HALLIWELL, M. A. G. & LYONS, M. H. (1985). *J. Appl. Cryst.* **18**, 446-451.

HORNSTRA, J. & BARTELS, W. J. (1978). *J. Cryst. Growth*, **44**, 513-517.

JAMES, R. W. (1967). *The Optical Principles of the Diffraction of X-rays*. London: Bell.

KERVAREC, J., BAUDET, M., CAULET, J., AUVRAY, P., EMERY, J. Y. & REGRENY, A. (1984). *J. Appl. Cryst.* **17**, 196-205.

KYUTT, R. N., PETRASHEN, P. V. & SOROKIN, L. M. (1980). *Phys. Status Solidi A*, **60**, 381-389.

LEE, P. (1981). *Opt. Commun.* **37**, 159-164.

PINSKER, Z. G. (1978). *Dynamical Scattering of X-rays in Crystals*. Berlin: Springer-Verlag.

PRINS, J. A. (1930). *Z. Phys.* **63**, 477-493.

SEGMÜLLER, A., KRISHNA, P. & ESAKI, L. (1977). *J. Appl. Cryst.* **10**, 1-6.

SPERIOSU, V. S. & VREELAND, T. JR (1984). *J. Appl. Phys.* **56**, 1591-1600.

TAKAGI, S. (1969). *J. Phys. Soc. Jpn*, **26**, 1239-1253.

TAUPIN, D. (1964). *Bull. Soc. Fr. Mineral. Crystallogr.* **87**, 469-511.

UNDERWOOD, J. H. & BARBEE, T. W. JR (1981). *Appl. Opt.* **20**, 3027-3034.

VARDANYAN, D. M. & MANOUKYAN, H. M. (1982). *Phys. Status Solidi A*, **69**, 475-482.

VARDANYAN, D. M., MANOUKYAN, H. M. & PETROSYAN, H. M. (1985). *Acta Cryst.* A**41**, 212-217.

ZACHARIASEN, W. H. (1945). *Theory of X-ray Diffraction in Crystals*. New York: Wiley.

Acta Cryst. (1986). A**42**, 545-552

Dynamical Diffraction Calculations for RHEED and REM

BY LIAN-MAO PENG AND J. M. COWLEY

Department of Physics, Arizona State University, Tempe, AZ 85287, *USA*

(*Received* 3 *January* 1986; *accepted* 27 *May* 1986)

Abstract

The multislice formulation of the many-beam dynamical diffraction theory has been applied to the Bragg case of electron diffraction for the extended surface of a perfect crystal and also for a crystal surface with a surface step. The wavefunctions within and outside the crystal have been calculated and used to derive the standing-wave pattern in the top atomic layers of the crystal, the intensities of the reflection high-energy electron diffraction (RHEED) pattern and the contrast of the reflection electron microscopy (REM) image. Calculations made for the diffraction of 19, 40 and 80 keV electrons from (111) surfaces of Pt and Au demonstrate the channeling of electrons under the conditions of surface resonance, the perturbation of the standing-wave field in the crystal by a one-atom-high surface step and the REM contrast

0108-7673/86/060545-08$01.50

for a through-focus series of images of a surface step. The method is applicable to models including surface relaxations and reconstructions and any kind of local defect of the surface or of the bulk crystal.

1. Introduction

Reflection high-energy electron diffraction (RHEED) and reflection electron microscopy (REM) have long histories of application under circumstances in which the experimental conditions have been poorly defined and the lack of an adequate theoretical basis for quantitative interpretation of intensities has, consequently, not been a serious limitation. This situation has been changed recently by the use of RHEED for the study of surfaces carefully prepared and adequately characterized by modern techniques of surface analysis (Menadue, 1972; Ino, 1980; Van Hove, Lent, Pukite & Cohen, 1983) and by the use of REM with sufficiently high resolution to show the configurations of atom-high steps on relatively clean flat surfaces (Osakabe, Tanishiro, Yaki & Honjo, 1980; Hsu & Cowley, 1983). It is therefore appropriate to reconsider the possibilities for calculating the diffraction amplitudes and image intensities for the reflection geometry. This must involve many-beam dynamical diffraction theory. It is necessary to include the treatment of faults and defects of the crystal since the reflection techniques are highly sensitive to deviations from the idealized case of a perfect crystal structure with a planar termination and the main applications of the techniques are for the study of such deviations.

Several theoretical approaches have been made to the calculation of RHEED intensities. The Bethe theory may be applied on the assumption of a three-dimensional periodic structure terminated by a plane. Modifications of the theory may be made in various ways to introduce deviations from the periodicity in the direction of the surface normal (Colella, 1972; Moon, 1972; Britze & Meyer-Ehmsen, 1978).

In an alternative type of approach (Masud & Pendry, 1976; Maksym & Beeby, 1981; Ichimiya, 1983) only a two-dimensional periodicity, parallel to the surface, is assumed. The crystal is considered to be cut into slices parallel to the surface and the wave function in different slices may be related by a transfer matrix. In this way changes in structure in the direction normal to the surface may be accommodated more readily. However, such approaches are not well adapted to deal with deviations from periodicity in directions parallel to the surface.

For transmission electron microscopy, calculations are made for defects either by making a column approximation or else by assuming that the defect is repeated periodically in directions perpendicular to the beam. For REM and RHEED with high-energy electrons, for which the incident beam is almost parallel to the surface, it is not particularly appropriate to make a column approximation by dividing the crystal into columns normal to the surface within which the crystal is considered to be perfect. Shuman (1977), who used such an approach to predict REM contrast for dislocations and stacking faults intersecting the surface, suggested that the resolution limit for the approximation is greater than 1000 Å in the beam direction. The other approach, which has been applied to treat surface steps (Kawamura & Maksym, 1985), is to assume that the surface defects form a periodic array so that the problem is reduced to that of dealing with a perfect crystal having a large periodicity in the beam direction. However, because of the small glancing angles of reflection, it is necessary to assume a very large periodicity in order to avoid serious overlap of the wave perturbations due to individual steps and this introduces computational difficulties.

In the approach which we describe here, the progressive modulation of the electron wave is simulated for transmission between slices taken almost perpendicular to the incident-beam direction. This is analogous to the transmission case except that the slices are essentially nonperiodic since they are made perpendicular to the crystal surface and include the wave function both inside and outside the crystal. An artificial large periodicity is composed by assuming that the whole crystal is repeated in the direction perpendicular to the face, as in Fig. 1.

The determination of the initial state of the electron wave function poses some difficulties. If the initial state is assumed to be a plane wave appropriately included so that its wave vector makes a small angle to the crystal surface of interest, the computation would simulate the case of illumination of the corner of a crystal, with a large part of the beam entering the crystal through a face almost perpendicular to the incident beam. This part of the beam would dominate the wave field in the crystal for a large distance

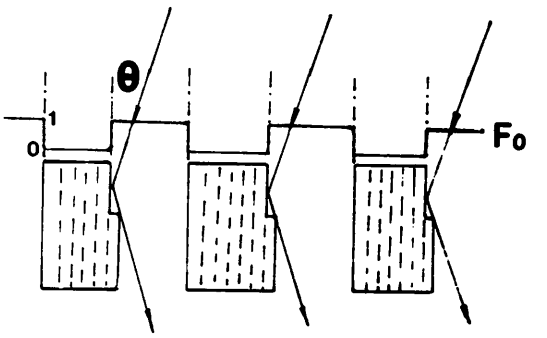

Fig. 1. Schematic diagram of the bases for calculation using the periodic continuation method. The fast electrons are incident on the stepped surface with glancing angle θ. The mask, F_0, prevents the irradiation of the top face of the crystal.

in the beam direction. In order to avoid this complication, a mask, F_0, is applied which transmits only that part of the incident beam which will strike the crystal face of interest. If the mask contains discontinuous transitions from 0 to 100% transmission it will introduce severe undesirable Fresnel diffraction effects. The transitions must therefore be made more gradual, by being 'rounded off' by a Gaussian. The model simulates the effect of a beam of finite width striking the crystal face at a glancing angle. The beam is at first all in the vacuum. The wave field in the crystal and the corresponding modulations of the wave in the vacuum are gradually generated as the electron wave is propagated in the beam direction, from slice to slice. After a certain distance a steady state will be reached and the wave field will then provide a good representation of the case of an infinite plane wave incident at a glancing angle on an infinite plane crystal surface. The effects of defects in the crystal structure or of imperfections on the crystal surface may then be explored by introducing changes in the nature of the slices in the model. Once the steady-state wave function for a perfect crystal is established for a particular crystal structure and angle of incidence, this may be used as the input wavefunction for consideration of the perturbations caused by any crystal defect or modification of the surface structure.

The model can be modified to represent, without any serious complication, the use of a non-planar incident wave such as that of a coherent convergent beam in a scanning transmission electron microscope (STEM). Since the slices are essentially non-periodic they can be made to represent any desired variation of structure in the direction perpendicular to the surface.

The method is based on the formulation of dynamical diffraction by Cowley & Moodie (1957), making use of the multislice computing methods which have been applied extensively in recent years for the calculation of transmission diffraction and imaging intensities. Some preliminary results obtained by use of this approach (Cowley & Warburton, 1969), applied to the simple case of a perfect single crystal face, showed some success. Using a more complete formulation and the more powerful computing techniques now available, we have demonstrated that this approach may be valuable for the exploration of dynamical diffraction processes at a surface, including the surface resonance effect, and the investigation of the effects of steps or other surface defects on the intensities of RHEED patterns or REM images.

2. Computing methods

The basis for the present calculations is the Cowley–Moodie multislice formulation of the many-beam dynamical diffraction theory (Cowley & Moodie, 1957). The computer programs used are based on those used by G. J. Wood and L. D. Marks for the simulation of high-resolution transmission electron microscopy (TEM) images and microdiffraction patterns. The slices of the specimen (thickness 2·9 Å or less) are taken to be perpendicular to the surface. The periodic continuation assumption (see Cowley, 1981) is made in order to deal with the essentially non-periodic object. The extended unit cell (dimensions 10×113 Å) includes the surface of interest, a sufficient thickness of crystal and the width of vacuum space needed to allow the incident and diffracted beams to enter and leave the model system without hindrance (Fig. 1). Because the content of the successive slices can be varied in an arbitrary fashion, it is possible to include any desired modifications of the structure in the beam direction, including surface steps or other surface or bulk defects.

Calculations have been made for the Pt (111) and Au (111) surfaces which have been investigated experimentally by Hsu & Cowley (1983). To include the influence of inelastic scattering on the elastic scattering, the scattering potential is taken as complex with the imaginary part equal to 10% of the real part. To include the effect of thermal vibrations of the atoms on the real part of the potential, the Fourier components of the potential are multiplied by a Debye–Waller factor. The number of sampling points in real space was $64 \times 1024 = 65\,536$ and the number of 'beams' in the output was 28 644.

The model used for the truncation of the crystal structure at the surface is the simplest possible one not having discontinuities. The potential distribution is the sum of the potential distributions for atoms which are not displaced from the bulk lattice positions, *i.e.* it is assumed that there is no surface 'relaxation' giving a variation of spacing of the planes of atoms parallel to the surface, and no 'reconstruction' to give a periodicity of the surface layer of atoms different from that of the bulk. Obviously calculations can be made in the future to incorporate the effects of both relaxation and reconstruction of the surface.

3. Results

3.1. *The wavefunction inside the crystal*

An advantage of the multislice method is that the wavefunction or intensity distribution of the wave may be obtained after each slice. It is therefore possible to investigate the building up of the wave field in the crystal as the beam enters the surface and propagates along the surface and the progressive modification of the wavefield following any defect or change of structure.

In Figs. 2 to 6 the wave-field intensity distributions are shown first for the wave near the entrance surface where most of the intensity is still in the vacuum

above the crystal and then at successive stages as the beam enters the crystal and establishes an equilibrium form. The build up of interference modulations is seen within the crystal and in the vacuum outside the crystal. It is the Fourier transform of the exit wave in the vacuum which gives the diffraction pattern and the transmission of this wave through the optical system of the electron microscope gives the wave function, and hence the intensity, of the REM image.

Two basic forms of excitation within a perfect crystal face have been found. These are illustrated in Figs. 2 and 3, calculated for the diffraction of 80 keV electrons from the Pt (111) surface with the incident-beam azimuth parallel to the [211] direction.

For Fig. 2 the incident beam is incident at a glancing angle of 39·6 mrad which corresponds to incidence at the 4·3 order of the 111 reflection in the absence of refraction effect or the 4·8 order if refraction with an inner potential of 32 V is taken into account. It is seen very clearly in Fig. 2 that a standing-wave field is established with maxima of intensity between the atomic places. Under these conditions it is expected that inelastic scattering of electrons by the atom cores will be minimized and there will be enhanced propagation of waves along the surface. The maximum between the top two surface planes is pronounced after 960 Å, Fig. 2(*b*), and then two and finally three maxima between planes (Fig. 2*b*) are established.

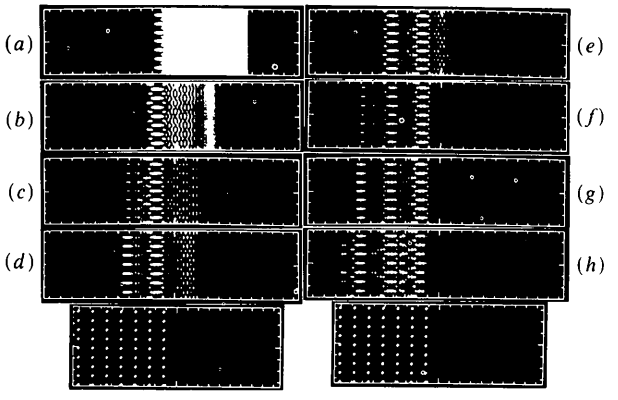

Fig. 2. Calculated wave functions for 80 keV electrons incident on the Pt (111) surface at a glancing angle of 39·6 mrad and [211] azimuth. The outputs are for distances from the entrance face of (*a*) 640, (*b*) 960, (*c*) 1120, (*d*) 1280, (*e*) 1440, (*f*) 1600, (*g*) 1760 and (*h*) 1920 Å. The atom positions are shown in the bottom diagrams.

For Fig. 3 the glancing angle of incidence is 23·6 mrad corresponding to incidence at the 2·6 order of the 111 reflection without refraction or the 3·4 order with refraction. The wave field is established in this case so that there are intensity maxima on or close to the atomic planes. In this case it is to be expected that the high concentration of electrons at the positions of the atom cores will lead to an enhancement of the inelastic scattering processes, an increased absorption effect and an increased intensity of secondary radiations (X-rays, Auger electrons).

For an intermediate angle of excitation, a different standing-wave configuration is generated, as in Fig. 4. The intensity distribution in this case can be constructed by a superposition of the intensity distributions of Figs. 2 and 3.

Applications of the production of standing-wave fields have been made for the X-ray diffraction case in the Bragg reflection configuration for the determination of particular atom positions on surfaces by detection of the characteristic X-ray emission (Cowan, Golouchenko & Robbins, 1980). The equivalent techniques using an incident electron beam and detection of characteristic X-ray or Auger electron emission are clearly feasible. The observation of the variation of X-ray emission with incident angle of an electron beam was observed and explained by Miyake, Hayakawa & Miida, (1968). The application for electron beams in the reflection mode for the location of atoms at surfaces would be the equivalent of the well known *ALCHEMI* technique (Spence & Taftø, 1983) which has been used in the transmission mode. Clearly calculations of the type illustrated in

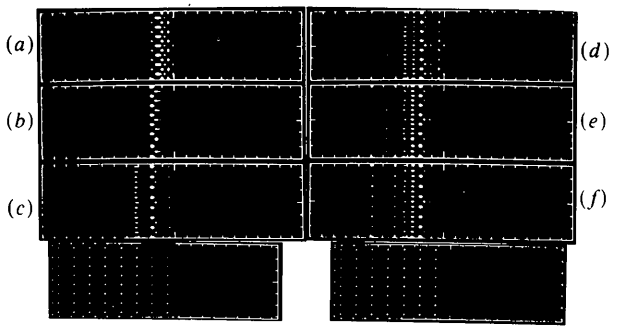

Fig. 3. Calculated wave functions for 80 keV electrons incident on the Pt (111) face at 23·6 mrad glancing angle at the [211] azimuth. Outputs are for distances from the entrance face of (*a*) 1280, (*b*) 1760, (*c*) 2240, (*d*) 2720, (*e*) 3040 and (*f*) 3168 Å. The atom positions are shown in the bottom diagrams.

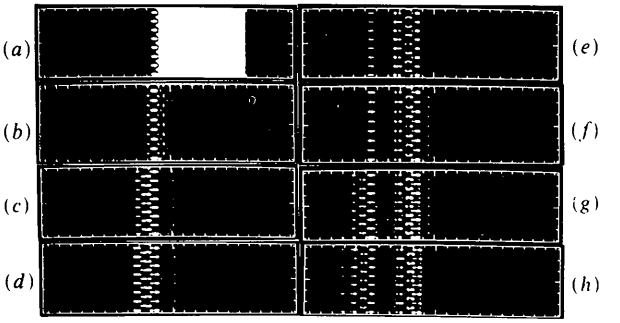

Fig. 4. As for Figs. 2 and 3, but with incident angle 28·4 mrad and outputs at (*a*) 800, (*b*) 1120, (*c*) 1440, (*d*) 1760, (*e*) 2080, (*f*) 2240, (*g*) 2400 and (*h*) 2560 Å.

Figs. 2 to 4 provide the necessary basis for interpretation of the observations of this type for the more general and powerful many-beam diffraction situations as well as for the two-beam diffraction situations which are normally considered.

3.2. *Perturbations of the wavefunction by a surface step*

The wave field established in a crystal under reflection diffraction conditions will be affected by any deviation from the perfect crystal model, *e.g.* by variations of the interplanar spacings at the surface due to lattice relaxation or by the presence of adsorbed layers of foreign atoms on the surface. It will be perturbed by any local imperfection, such as a defect on the surface or in the crystal, and by any associated strain field. Here we consider only the case of a step on the surface for the idealized case of no relaxation and no associated strain field.

Fig. 5 shows the results of calculations for a step on the Pt (111) surface. The step is one atom high, perpendicular to the incident beam, and is a step up when viewed from the incident-beam direction. The results show the wave field being established in the perfect crystal and then being affected by the step at Fig. 5(*e*). The presence of the step modifies the wave field initially only for the atomic places which are close to the surface (Figs. 5*g* and *h*) but the modification gradually extends further into the crystal. The new equilibrium, perfect-crystal wave field is established for the top two atomic planes by Fig. 5(*j*) but the wave field is still strongly perturbed for the third and fourth atomic layers.

It seems probable that the RHEED intensities and REM contrast will be affected most strongly by the perturbation of the wavefield in the top two atomic layers. Hence it is expected that the distance over which the image intensity will be strongly modified will be that corresponding to the distance between Figs. 5(*e*) and (*j*) in this case, *i.e.* a distance of about 400 Å in the beam direction. When the foreshortening factor is taken into account, this gives a line width for in-focus REM images which is consistent with the observations.

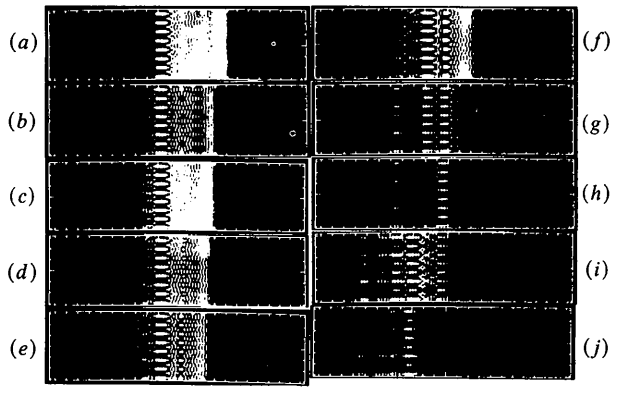

Fig. 5. Calculated wave functions for 19 keV electrons incident on the Pt (111) face at the [211] azimuth with a glancing angle of incidence of 50·3 mrad. There is a step one atom high at 488 Å from the entrance face. Output for distances (*a*) 352, (*b*) 416, (*c*) 432, (*d*) 448, (*e*) 464, (*f*) 480, (*g*) 544, (*h*) 640, (*i*) 736 and (*j*) 832 Å.

3.3. *Surface resonance effects*

By combining the results of the calculation of the wave function in the crystal with the calculation for the RHEED intensities it is possible to determine the origin of the various effects which have been observed in the diffraction patterns. Here we consider the origin of the well-known surface resonance effect.

The intensity anomalies, or strong modifications of particular diffraction spots, attributed to surface resonance have been studied for many years in RHEED and also in LEED. The resonance effect usually occurs when the specular reflection spot coincides with a Kikuchi line. Miyake, Kohra & Takagi (1954) recognized this to be a beam threshold effect and pointed out that the coincidence of the specular reflection with Kikuchi line indicates a particular diffraction condition for which (1) the Bragg condition is fulfilled for a certain lattice plane, and (2) the Bragg diffracted beam is propagating in a direction nearly parallel to the surface (see Marten & Meyer-Ehmsen, 1985).

Later, Kohra, Moliere, Nakano & Ariyama (1962) related the beam threshold condition, (2), to the existence of a wave field which is confined to the surface region of the crystal. More recently, Marten & Meyer-Ehmsen (1985), using the dynamical RHEED theory of Maksym & Beeby (1981), have shown that the enhancement of the specular beam intensity can be attributed to the scattering from the topmost atomic layer on the surface. They concluded that there are resonances by which the electrons are efficiently coupled to states for which the electrons are channeled along paths parallel to the surface and are confined to the potential troughs of the first monolayer of atoms on the surface.

Our calculations are made for the Pt (111) surface with 19 keV electrons incident at a glancing angle of 54·1 mrad and the beam azimuth in the [110] direction. The results are shown in Figs. 6 and 7. The calculated diffraction pattern, Fig. 6, shows the strong Laue circle of reflections with the 3·5 order of the 111 reflection at the specular reflection position and the 004 and $33\bar{1}$ and 440 reflections almost parallel to the plane of the surface. Fig. 7 shows the development of the wave functions and the corresponding current density distributions projected on the surface normal.

From Fig. 7 it is evident that the wave function is concentrated near the surface and that strong maxima of the electron current density occur at the position

of the topmost layer of atoms. Diffraction from this wave function distribution into the vacuum then gives the strong diffracted beams parallel to the surface in Fig. 7 and strongly enhanced specular reflection. The results thus confirm the existence of the surface channeling effect and illustrate the occurrence of the 'monolayer resonance'.

3.4. *Surface step contrast in REM*

Steps on the surfaces of crystals, one atom high, have been observed with high contrast by several groups using REM in both the high-vacuum electron microscopes (Osakabe, Tanishiro, Yagi & Honjo, 1980) and in commercial elctron microscopes having relatively poor vacuum (Hsu & Cowley, 1983). The contrast of the step image has been shown to vary with the direction of the incident beam and with the position of the objective aperture of the imaging system.

Elementary considerations suggest two or more possible origins for the step contrast. Phase contrast, resulting from the difference in phase between waves diffracted from the top and bottom of the step, is expected to give characteristic black–white contrast for out-of-focus images. For small phase difference, the phase contrast will go to zero for the in-focus condition. If there is a strain field in the crystal associated with the surface step, the resultant variations of the lattice-plane orientations will give diffraction contrast.

It is shown by Cowley & Peng (1985) that the main features of the observed contrast could be accounted for by a simple theory, including phase contrast for the larger phase differences which are expected to occur but not taking into account any strain fields. This theory gave a good account of the dependence of the contrast on defocus, incident-beam direction and objective aperture position.

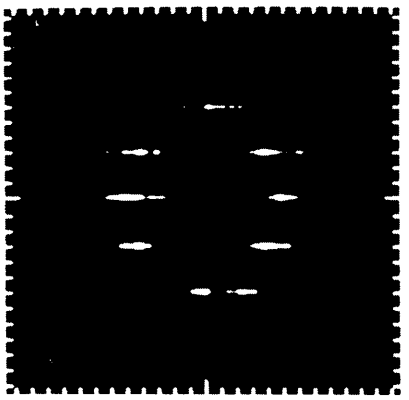

Fig. 6. The diffraction pattern corresponding to the wave leaving the crystal at 406 Å in the case of Fig. 7. The specular reflection (the 3·5 order of the 111) is on the right. The 004 is at the top and the $33\bar{1}$ and 440 are at the bottom. The pattern includes both the vacuum and the crystal waves.

Simple theories of this sort, however, are based on a column approximation which assumes that the wave amplitude at a point on the surface is determined only by the content of a narrow column of the crystal directly below that point. The implications of our calculations, such as those of Fig. 5, are that the perturbation of the wave field due to a surface step may extend for hundreds of ångströms along the crystal surface in the beam direction. Hence the use of a column approximation must give a very poor representation of the image contrast for high-resolution imaging conditions. An adequate calculation of image contrast can be made only by use of many-beam dynamical diffraction theory with no column approximation.

We have made calculations of the contrast for steps on an Au (111) surface for the idealized case of no surface relaxation and no strain field in the crystal. The beam is assumed to be incident at a glancing angle of 28 mrad which corresponds to the 333 reflection from the (111) surface planes. The beam azimuth is [110] and the surface steps are assumed to be perpendicular to the beam. An objective aperture of size $0{\cdot}18\ \text{Å}^{-1}$ is assumed to be centered on the specular reflection spot, and the spherical aberration

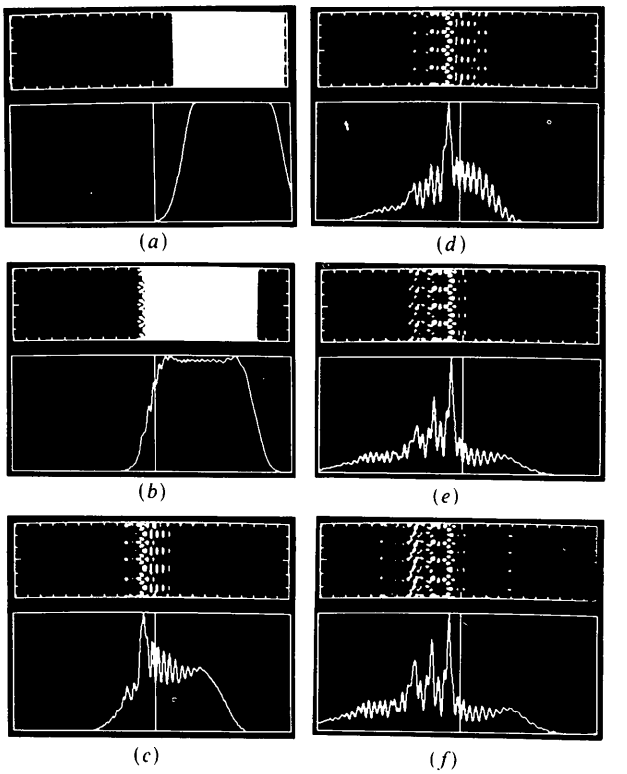

Fig. 7. The calculated wave functions and projected current density distributions for 19 keV electrons incident on a Pt (111) surface with [110] azimuth and glancing angle of incidence 54·1 mrad. Output for distances (*a*) 2·9, (*b*) 87, (*c*) 174, (*d*) 290, (*e*) 364 and (*f*) 406 Å.

constant for the objective lens is assumed to be 1·2 mm.

Fig. 8 shows a through-focus step. The field of view in each case is limited in width by the dimensions of the model assumed in the calculations (Fig. 1) and is chosen to be just large enough to include the main features of the intensity profile of the image.

The images show the characteristic black–white contrast for the out-of-focus conditions. For the under-focus condition, Fig. 8(*a*), the broad white–black line pair is strong. As the defocus decreases the white–black pair becomes sharper and the black line (low intensity) becomes dominant (Figs. 8*b* and *c*). At about the Scherzer defocus condition (optimum focus for TEM imaging) there is only a sharp dark line. Then for over-focus the reverse-contrast black–white line pair appears and becomes broader. All of these features are in agreement with the prediction of the simple theory (Cowley & Peng, 1985) and with the observations.

The computing method thus provides a basis for the quantitative prediction of REM contrast of surface steps which can be extended to the examination of the effects of the various experimental parameters (wavelength, glancing angle of incidence, azimuth, objective aperture position) for various models of the surface step configuration, including the effects of relaxation, strain fields or foreign atoms absorbed on the step.

4. Concluding remarks

The preliminary results presented here amply demonstrate that the multislice formulation of the dynamical diffraction theory provides a useful basis for calculations for the Bragg case of diffraction from a surface. It allows the calculation of the wave field both inside and outside the crystal for any model of the crystal surface and for the perturbations of the wave field resulting from any local defect. From the calculated wave field within the crystal can be derived the electron current density distribution in relation to the atom positions. This can reveal the presence of channeling effects and can provide predictions of the variation of intensities of secondary radiation generated as a result of inelastic scattering processes.

From the calculated wave field in the vacuum it is possible to derive the intensities of the diffraction pattern or of the image of the crystal surface.

In these exploratory calculations we have confined our attention to idealized simple models for the crystal surface and for the steps on the surface. There are no inherent difficulties in the inclusion of surface relaxations or reconstructions or in the treatment of other types of surface or bulk defects such as foreign atoms or crystallites in, or on, the surface, stacking faults intersecting, or parallel with, the surface, and so on.

The principal limitation of the method at this stage is that, because the computations are rather large, it is difficult to explore adequately the effects of varying all the various experimental parameters for the wide range of possible models of the surfaces and their defects. However, this difficulty will no doubt be alleviated by experience with a variety of calculations and the method is seen as a promising approach to the adequate theoretical description of RHEED and REM observations.

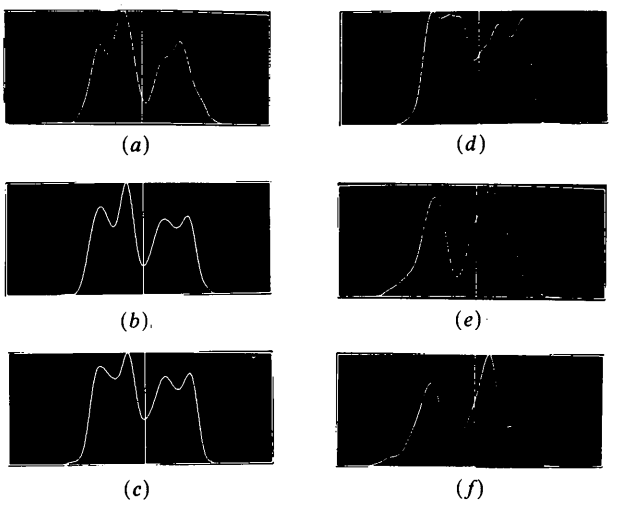

Fig. 8. Calculated intensity profiles for REM images of a surface step for 40 keV electrons incident on an Au (111) face in [110] azimuth with incident angle 28 mrad using the wave at the exit face after thickness 1960 Å. Defocus values are (*a*) −2800, (*b*) −1800, (*c*) −1200, (*d*) −400, (*e*) +2000 and (*f*) +2600 Å.

We are grateful to Drs G. J. Wood and L. D. Marks who provided the original computer programs for the multislice calculations. This work was supported by NSF grants DMR7926400 and DMR8510059 and made use of the resources of the ASU Facility for High Resolution Electron Microscopy supported by NSF grant DMR8306501.

References

BRITZE, K. & MEYER-EHMSEN, G. (1978). *Surface Sci.* **77**, 131–141.
COLELLA, R. (1972). *Acta Cryst.* A**28**, 11–15.
COWAN, P. L., GOLOUCHENKO, J. A. & ROBBINS, M. F. (1980). *Phys. Rev. Lett.* **44**, 1680–1683.
COWLEY, J. M. (1981). *Diffraction Physics*, 2nd ed., pp. 243–245. Amsterdam: North Holland.
COWLEY, J. M. & MOODIE, A. F. (1957). *Acta Cryst.* **10**, 609–619.
COWLEY, J. M. & PENG, L. M. (1985). *Ultramicroscopy*, **16**, 59–67.
COWLEY, J. M. & WARBURTON, P. M. (1969). In *The Structure and Chemistry of Solid Surfaces* edited by G. A. SOMORJAI. New York: Wiley.
HSU, T. & COWLEY, J. M. (1983). *Ultramicroscopy*, **11**, 239–250.
ICHIMIYA, A. (1983). *Jpn. J. Appl. Phys.* **22**, 76–180.
INO, S. (1980). *Jpn. J. Appl. Phys.* **19**, 1277–1290.
KAWAMURA, T. & MAKSYM, P. A. (1985). *Surface Sci.* **161**, 12–24.

KOHRA, K., MOLIERE, K., NAKANO, S. & ARIYAMA, M. (1962). *J. Phys. Soc. Jpn*, **17**, Suppl. BII, 82-87.
MAKSYM, P. A. & BEEBY, J. L. (1981). *Surface Sci.* **110**, 423-438.
MARTEN, H. & MEYER-EHMSEN, G. (1985). *Surface Sci.* **151**, 570-584.
MASUD, N. & PENDRY, J. B. (1976). *J. Phys. C*, **9**, 1833-1844.
MENADUE, J. F. (1972). *Acta Cryst.* A**28**, 1-11.
MOON, A. R. (1972). *Z. Naturforsch. Teil A*, **27**, 390-395.
MIYAKE, S., HAYAKAWA, K. & MIIDA, R. (1968). *Acta Cryst.* A**24**, 182-191.
MIYAKE, S., KOHRA, K. & TAKAGI, M. (1954). *Acta Cryst.* **7**, 393-401.
OSAKABE, N., TANISHIRO, Y., YAGI, K. & HONJO, G. (1980). *Surface Sci.* **97**, 393-408.
SHUMAN, H. (1977). *Ultramicroscopy*, **2**, 261-269.
SPENCE, J. C. H. & TAFTØ, J. (1983). *J. Microsc. (Oxford)*, **130**, 147-154.
VAN HOVE, J. M., LENT, C. S., PUKITE, P. R. & COHEN, P. I. (1983). *J. Vac. Sci. Technol. B*, **1**, 741-746.

Acta Cryst. (1986). A**42**, 552-559

Dynamical Theory of Diffraction on a Periodic System of Point Scatterers

BY O. LITZMAN

Department of Theoretical Physics and Astrophysics, Faculty of Science of UJEP, Kotlářská 2, 611 37 *Brno, Czechoslovakia*

(*Received* 28 *January* 1986; *accepted* 20 *June* 1986)

Abstract

Ewald's self-consistent field method is used to deduce formulae for the reflection and transmission coefficients of a crystal slab in a well arranged determinant form. No supposition concerning the magnitude of the interaction between the diffracted particles and the crystal or the number of diffracted beams is made.

1. Introduction

The diffraction of radiation on a system of scatterers is encountered in many branches of physics: let us mention the diffraction of X-rays, electrons or neutrons on a crystal or the classical diffraction of visible light on a system of small metal particles embedded in a dielectric - low-energy photodiffraction, LEPD (Ohtaka, 1980). The problem of multiple scattering is rather difficult in both classical and quantum physics. That is why different approximations are used. In the kinematical theory multiple scattering is neglected. In some dynamical theories the interaction of the radiation with the crystal is supposed to be small, the diffraction is studied in the neighbourhood of the Bragg diffraction angle, in the two-beam approximation *etc.* But the interaction is not small either in low-energy electron diffraction (LEED) or in LEPD; then computers are needed to process general formulae.

There is one case in which multiple scattering leads to relatively well arranged and simple algebraic equations - multiple scattering on point scatterers. The problem of point scatterers in quantum mechanics has been handled from the general point of view, *e.g.* by Demkov & Ostrovskij (1975). In solid-state physics the model of point scatterers is adequate in neutron diffraction, soft X-ray diffraction (Henke, Lee, Tanaka, Shimabukuro & Fujikawa, 1982), in LEED in a strong limited *s* approximation or in LEPD, if the diameter of the embedded particles is sufficiently small compared with the wavelength of the photon.

In our earlier papers we were engaged in Ewald's dynamical theory of X-ray diffraction on a simple periodic lattice (without basis) (Litzman, 1980; Litzman & Rózsa, 1980). The results have been used in the soft X-ray optics of thin films (Litzman & Šebelová, 1985). The aim of this paper is to deduce formulae for the reflection and transmission of radiation by a system of point scatterers forming a general lattice (with a basis). Neither a small interaction between the radiation and scatterers nor a two-beam approximation nor proximity to the Bragg diffraction angle is assumed. On the other hand we confine ourselves to scalar waves, *i.e.* to solutions of the Schrödinger equation. Vector waves (electromagnetic waves) can be handled in a similar way, the corresponding matrices being, roughly speaking, three times greater. Thus, for electromagnetic waves we confine ourselves to hints at relevant points.

2. Basic formulae

We shall study the diffraction of particles (electrons, neutrons) on a system of point scatterers, fixed at the lattice points of an ideal crystal slab with *s*

0108-7673/86/060552-08$01.50